

Epidemic spreading on spatial networks with distance-dependent connectivity

Matúš Medo^{1,2}

¹*Department of Radiation Oncology, Inselspital, University Hospital of Bern, and University of Bern, 3010 Bern, Switzerland*

²*Department of Physics, University of Fribourg, 1700 Fribourg, Switzerland**

We study the epidemic spreading on spatial networks where the probability that two nodes are connected decays with their distance as a power law. As the exponent of the distance dependence grows, the resulting networks smoothly transition from the random network limit to the regular lattice limit. We show that despite keeping the average number of contacts constant, the increasing exponent hampers the epidemic spreading as it makes long-distance connections less frequent. The growth of the number of infections is also influenced by the exponent value and changes from exponential growth to power-law growth. The resulting growth is compatible with recent analyses of the COVID-19 spreading in most countries.

I. INTRODUCTION

Mathematical modeling of epidemic processes has a long tradition [1–3]. After the rise of the network science [4, 5], the study of epidemics spreading on networks has inevitably led to a flourishing of literature [6–9]. Besides research focusing on the impact of hubs [10], long-distance connections [11], and the effective spreading geometry [12], the efforts addressing epidemics spreading on spatial networks with prevailing short connections are comparatively few. This is a research gap that calls to be addressed in the face of the current uncontrolled spreading of the virus COVID-19 [13] an ever-increasing number of countries introduce unprecedented movement and activity restrictions.

We study here epidemic spreading on model spatial networks introduced in [14] where a single parameter can be used to gradually shift from a random network limit where long connections are common to a regular lattice limit where only the nearest-neighbors are connected. In close similarity with the classical Watts-Strogatz model [15], small-world networks (networks with high clustering and small average distance between the nodes) are produced for intermediate values of the parameter. From the point of view of epidemics spreading, the two parameter limits are well understood, leading to exponential growth of the number of infections when long links prevail and quadratic growth when they are absent [16]. To explore and understand how exponential epidemic growth gradually changes in power-law growth is the main goal of this study.

II. A SPATIAL NETWORK MODEL

In a spatial complex network, the probability that two nodes are connected is given by the distance between them [7]. We use here the model introduced in [14] where

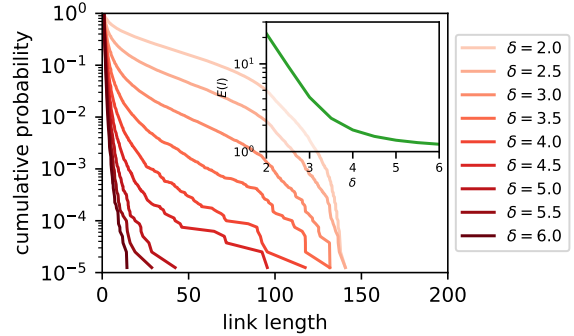


FIG. 1. The distribution of link lengths in model spatial networks with $N = 40,000$. For each δ , λ is chosen to achieve the chosen mean degree $z = 4$. Note that for this N , the longest possible link is $\sqrt{N}/\sqrt{2} \approx 141$. The inset shows the mean link length, $E(l)$, as a function of the exponent δ .

N nodes form a two-dimensional square lattice with periodic boundary conditions; we assume for simplicity that $N = S^2$ where S is a natural number. In this model, the probability that two nodes are connected depends only on their distance d , hence the label “network with distance-dependent connectivity”, as

$$P(d) = \frac{1}{1 + \lambda d^\delta} \quad (1)$$

where λ and δ are model parameters. The exponent δ determines how fast $P(d)$ decays with distance and λ can be used to achieve a desired mean degree, z , in the resulting network. In [14], the authors show that $2.5 \gtrsim \delta \lesssim 3.5$ produces small-world networks where the average shortest paths are “short” and the clustering coefficient values are high. Figure 1 shows that as δ grows, links in model networks become shorter. In the limit $\delta \rightarrow \infty$, only the shortest links are possible and the network becomes regular: each node is connected with its z closest neighbors. The opposite limit, $\delta \rightarrow 0$, is also instructive: node distance then becomes irrelevant and the connection probability is the same, $1/(1 + \lambda)$, for all nodes. We thus recover a classical random network [17].

* matus.medo@unifr.ch

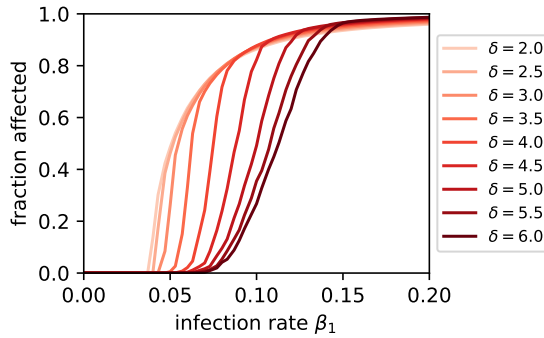


FIG. 2. The fraction of infected nodes at $t = 300$ for $N = 40,000$ and $z = 4$ as a function of the infection rate. The values shown here are median values over 100 realizations of the epidemic process.

III. AN EPIDEMIC MODEL

We use here an SEIR epidemic model [2, 18] where each node can be in one of four possible states: susceptible (S), exposed (E), infected (I), and recovered (R). While the choice of the model and its parameters are motivated by the ongoing COVID-19 epidemic, the presented findings do not change qualitatively when a different model or a different set of parameters are used.

All nodes are initially susceptible except for one node which is exposed. The exposed nodes represent the individuals who have already contracted the disease but have not developed the symptoms yet. In the case of COVID-19, these individuals have been shown to considerably contribute to spreading the disease [19]. The simulation runs in time steps with one step representing one day. If susceptible node i is connected with an exposed node, the probability that node i becomes exposed is β_1 . If susceptible node i is connected with an infected node, the probability that node i becomes exposed is β_2 .

While the infection process is probabilistic, we assume for simplicity that the disease progression is deterministic: If node becomes exposed at time t , it automatically becomes infected (develops disease symptoms) at time $t + T_1$ and recovered at time $t + T_1 + T_2$. Here T_1 is the incubation period and T_2 is the recovery time. Recovered nodes cannot contract the disease again.

We use $T_1 = 5$, $T_2 = 14$, and $\beta_2/\beta_1 = 0.2$ (this reflects the role of asymptomatic agents in the spreading process [19]). We simulate 300 time steps of the epidemic spreading. We run 100 independent realizations of the epidemic process and use the median to find a representative epidemic outcome at any time point. We measure the epidemic spreading using the number of affected nodes which includes exposed, infected and recovered nodes, so it is naturally a cumulative metric which quantifies how many nodes have contracted the disease during the simulation time.

IV. EPIDEMIC DYNAMICS ON THE SPATIAL NETWORKS

We present here results of numerical simulations of epidemic spreading on model spatial networks. Before addressing the dynamics of the epidemic process, Figure 2 shows that the spatial distribution of links, controlled in the model by the exponent δ , has strong influence on the epidemic spreading. In particular, the fraction of infected nodes at a given time decreases as δ grows. This implies that the epidemic spreading can be effectively reduced by both social distancing which is now widely used during the COVID-19 epidemic (in the scope of our model, social distancing reduces the mean node degree) as well as by purposely choosing nearby contacts. In other words, a higher number of strongly localized social contacts can lead to the same fraction of infected population as a lower number of widely distributed social contacts. Besides the mathematical aspects, localized social contacts make contact tracing easier.

The effect of δ can be readily understood by inspecting the spreading patterns for various values of δ shown in Figure 3. When δ is high ($\delta = 6$), the epidemic spreads as on a regular lattice and develops a clearly-defined spreading front. Nodes on the front that can spread the infection further can then spread it in only one direction (outwards) which limits their effective reproduction number (number of nodes that they infect on average). As δ decreases, the spreading front first becomes “diffuse” ($\delta = 4$) until it “dissolves” entirely ($\delta = 2$). The epidemic then spreads more effectively as it is more probable that a neighbor of an infected nodes is susceptible to the infection.

We now return to the main question: the effect of the spatial network structure on the dynamics of epidemic spreading. This dynamics has two well known special cases. On a random contact network, the assumption of homogeneous mixing of susceptible and infected nodes is valid and one recovers the infamous exponential epidemic growth [2]. On a regular two dimensional lattice with nearest-neighbor connections, the epidemic spreading instead develops an epidemic front that propagates at a constant velocity. The front’s constant velocity then directly implies that the radius of the affected area grows linearly with time and, consequently, the number of infected individuals grows quadratically with time [16].

Spatial networks with distance-dependent connectivity give us the possibility to smoothly transition between the two extremes. We can thus directly observe how quadratic growth at high δ values changes in exponential growth at low δ values. Figure 3 provides the first indication with the epidemic front becoming more diffuse and the speed of its propagation grows as δ decreases. As this happens, the argument leading to quadratic growth ceases to be valid and we expect the growth to be faster than quadratic. This is confirmed by Figure 4 where we show the epidemic dynamics for various contact networks. Growth that is of a power-law kind (it follows a

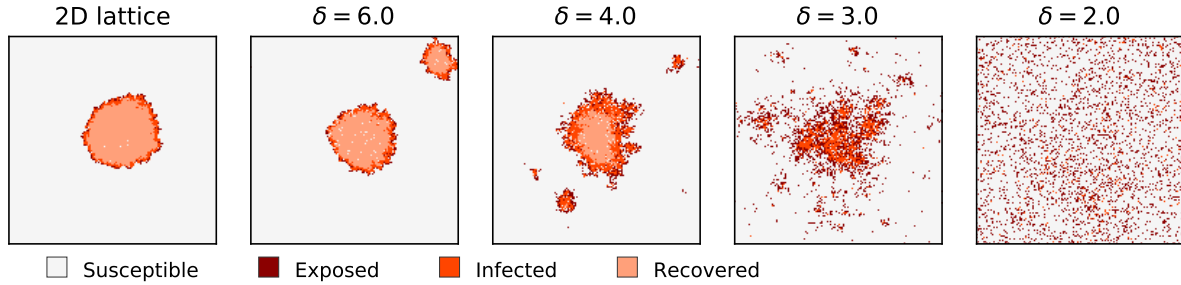


FIG. 3. Epidemic spreading on model the square lattice and spatial networks with various values of the exponent δ . We use $N = 160,000$ and $z = 4$. The snapshots are taken when 10% of all nodes have been affected by the epidemic. We use here $\beta_1 = 0.16$ for which half of all nodes becomes affected at the end of simulation for $\delta = 6$.

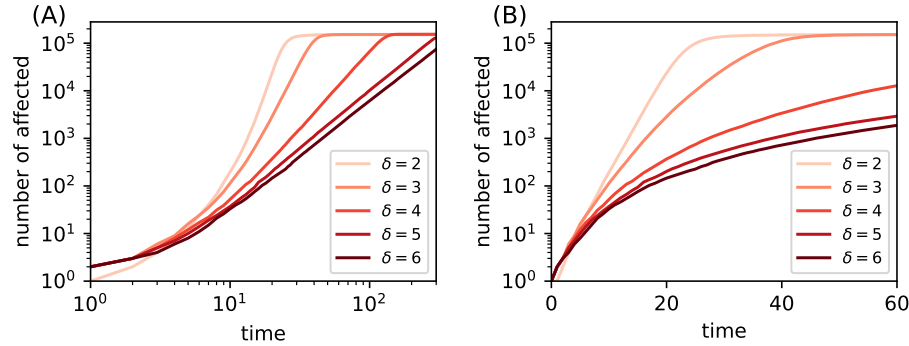


FIG. 4. Time evolution of the number of affected nodes for various contact networks. Straight lines in the log-log panel (A) are indicative of power-law growth. Straight lines in the log-linear panel (B) are indicative of exponential growth. As in Figure 3, we use $N = 160,000$, $z = 4$, and $\beta_1 = 0.16$.

straight line over a substantial part of the log-log plane in panel A) for the 2D lattice as well as for the spatial networks with $\delta \gtrsim 4$ becomes clearly exponential for the random network and for the spatial network with $\delta = 2$ (see the straight lines in the log-linear panel A).

We find that quadratic epidemic growth on 2D lattices generalizes to power-law growth on the model spatial networks with sufficiently high exponent δ . Table I shows that for the data shown in Figure 4A, stable estimates of the growth exponent (indicating good power-law fits of the data) can be obtained for δ greater or equal to 4. The resulting power-law growth exponents supported by simulations with $N = 160,000$ nodes lie in the range 2–3.25. As N grows, the range of δ where a power-law fits the data well seems to expand. The results obtained on random networks and the regular square lattice (not shown) are very close to the displayed results for $\delta = 2$ and $\delta = 6$, respectively. Notably, the power-law exponent is not exactly two even for the square lattice. This is due to the probabilistic nature of the spreading that results in non-vanishing randomness of the spreading front that can be well seen in the first panel of Figure 3. Finally, note that the mechanisms leading to power law growth of the number of infections studied here are very different from those studied in [20] where a diverging second

TABLE I. Power-law exponents, \hat{b} , estimated by fitting straight lines to the data in Figure 4A. To focus on the straight part of the dependencies, we fit only the values below $N/2$ infected cases and above $100 - 800$ infected cases. The reported ranges of the fitted exponents correspond are obtained by varying the lower bounds. The exponent estimate for $\delta = 3$ varies in a comparatively broader range, indicating that power-law growth is not a good fit in this case.

δ	3	4	5	6
\hat{b}	5.26–5.59	3.23–3.26	2.39–2.41	2.28–2.30

moment of the degree distribution was the main reason for deviating from the exponential spreading pattern. In our case, by contrast, the degree distribution is narrow (Poissonian) even when it can be made broad by modifying the network model [21].

The observed power-law growth with δ -dependent exponents matches the recent observations of the COVID-19 spreading in a power-law fashion. After the first reports based on data from China [22, 23], similar results have been recently reported for nearly all countries where COVID-19 spreads [24]. Our results suggest that in the times of social distancing, the contact networks can be

modeled as spatial networks with a relatively high exponent of the connecting probability decay.

V. DISCUSSION

In this work, we studied the interplay between the functional form of the connection probability in spatial networks and the dynamics of epidemic spreading on them. There are two main findings. Firstly, short (localized) links hinder the epidemic. We can thus achieve a better outcome (fewer infections, slower growth) by avoiding distant contacts even if the mean number of contacts remains fixed. Secondly, when short links are frequent in the network, the number of infected individuals grows as a power-law instead of the canonical exponential epidemic growth. In the framework of the chosen connection probability probability decaying with node distance as a power law, frequent short links are achieved when the exponent of the connection probability decay is high. In our simulations, power law growth of the number of infections emerges when this decay exponent is at least four. This observation is particularly relevant as the latest data show that the COVID-19 spreading in most

countries indeed follows a power-law pattern instead of exponential growth. In other words, our results suggest that the social contacts over which the virus spreads are now extraordinary short which helps us to avoid the exponential spreading and thus give us more time for necessary actions.

To better understand the impact of various features of the contact network on the resulting epidemic spreading, several modifications and generalizations of the network model can be studied in the future: (1) replacing individual nodes with households where each node has local connections to all other household members and distance-dependent connectivity is only used to model the connections across the households, (2) introducing link weights that represent the intensity of the social contact and naturally play a role in the disease transmission, (3) introducing degree heterogeneity to reflect that even under social distancing, some nodes inevitably have considerably more contacts than the average, and others. Finding an analytical relation between the connectivity decay exponent δ and the epidemic growth exponent and formulating effective differential equations that describe the epidemics dynamics on spatial networks are other important directions.

[1] W. O. Kermack and A. G. McKendrick, *Proceedings of the Royal Society of London, Series A* **115**, 700 (1927).

[2] O. Diekmann and J. A. P. Heesterbeek, *Mathematical epidemiology of infectious diseases: Model building, analysis and interpretation*, Vol. 5 (John Wiley & Sons, 2000).

[3] F. Brauer, *Infectious Disease Modelling* **2**, 113 (2017).

[4] A.-L. Barabási *et al.*, *Network science* (Cambridge University Press, 2016).

[5] M. Newman, *Networks* (Oxford University Press, 2018).

[6] M. J. Keeling and K. T. Eames, *Journal of the Royal Society Interface* **2**, 295 (2005).

[7] M. Barthélémy, *Physics Reports* **499**, 1 (2011).

[8] R. Pastor-Satorras, C. Castellano, P. Van Mieghem, and A. Vespignani, *Reviews of Modern Physics* **87**, 925 (2015).

[9] M. A. Porter and J. P. Gleeson, *Frontiers in Applied Dynamical Systems: Reviews and Tutorials* **4** (2016).

[10] R. Pastor-Satorras and A. Vespignani, *Physical Review E* **63**, 066117 (2001).

[11] D. Balcan, V. Colizza, B. Gonçalves, H. Hu, J. J. Ramasco, and A. Vespignani, *Proceedings of the National Academy of Sciences* **106**, 21484 (2009).

[12] D. Brockmann and D. Helbing, *Science* **342**, 1337 (2013).

[13] W. H. Organization *et al.*, (2020).

[14] M. Medo, *Physica A: Statistical Mechanics and its Applications* **360**, 617 (2006).

[15] D. J. Watts and S. H. Strogatz, *Nature* **393**, 440 (1998).

[16] S. Riley, K. Eames, V. Isham, D. Mollison, and P. Trapman, *Epidemics* **10**, 68 (2015).

[17] B. Bollobás and B. Béla, *Random graphs* (Cambridge University Press, 2001).

[18] H. W. Hethcote, *SIAM Review* **42**, 599 (2000).

[19] R. Li, S. Pei, B. Chen, Y. Song, T. Zhang, W. Yang, and J. Shaman, *Science* (2020).

[20] A. Vazquez, *Physical Review Letters* **96**, 038702 (2006).

[21] M. Medo and J. Smrek, *The European Physical Journal B* **63**, 273 (2008).

[22] A. Brandenburg, arXiv preprint arXiv:2002.03638 (2020).

[23] A. L. Ziff and R. M. Ziff, *medRxiv* (2020), [10.1101/2020.02.16.20023820](https://doi.org/10.1101/2020.02.16.20023820), <https://www.medrxiv.org/content/early/2020/03/03/2020.02.16.20023820>.

[24] R. Kollar and K. Bodova, Unpublished.